RSC Advances

ROYAL SOCIETY OF CHEMISTRY

www.rsc.org/advances

RSC Advances

RSCPublishing

COMMUNICATION

Gentle Reduction of SBA-15 Silica to its Silicon Replica with Retention of Morphology

Cite this: DOI: 10.1039/x0xx00000x

Xiulei Ji,[a†] Guang He[a], Carmen Andrei,[b] and L.F. Nazar[a*]

Received ooth October 2013,
Accepted ooth January 20xx

DOI: 10.1039/x0xx00000x

www.rsc.org/

We report the transformation of mesoporous silica to its silicon replica with maintenance of structural regularity. The method employs mild displacement reactions with Mg intermetallics as the source of Mg vapor at low partial pressure. The mild conditions aid in high fidelity replication of the nanoporous framework of the starting silica.

Ordered mesoporous materials have been the subject of remarkable focus in the last two decades owing to their unique properties,[1] although few elemental materials have been shown to adopt such morphology. On the other hand, nanostructured silicon materials have attracted attention due to their potential energy applications including the conversion of solar[2] and thermal[3] energy into electrical energy and high density energy storage, *i.e.* as the negative electrodes in Li ion batteries.[4] Top down and bottom up fabrication strategies have been developed for silicon materials with 0D[5], 1D[6] and porous 3D[7,8] morphologies, but most typically require very expensive silicon precursors. In industry, metallurgical silicon is extracted from high purity silica by a carbothermal reduction reaction carried out well above 1500°C.[9] Long known metallothermic methods[10] have recently attracted attention as a viable route to nanoscaled versions of silicon materials. The pioneering work by Sandhage *et al.* used Mg vapour to reduce micron sized silica diatom frustules to their silicon replicas in a vacuum reactor.[–11] The silicon exhibits a domain size of 13 nm within the walls of the macroporous replica. Both unreacted silica and the over-reduction product, Mg_2Si, remain in the product. To circumvent this problem, Maier *et al.* reported reaction of a mixture of Mg powder and mesoporous SiO_2 under Ar/H_2 at high temperature. [12] This approach improved the homogeneity of the reaction although mesoporous silica was converted to macroporous silicon. Unreacted silica remained owing to Mg vapour loss in the reaction container, illustrating the challenge: in order to force silica reduction to completion, Mg in substantial excess is required. This reacts with the just-synthesized silicon at the high temperatures generated by the exothermic reaction, leading to degradation of the structure owing to the formation of Mg_2Si, and to collapse of porosity on the nano or meso scale. This can be inhibited by carrying out the magnesiothermic reaction in the presence of carbon, as recently demonstrated by Stucky *et al.* who converted long-range ordered SiO_2 into its mesoporous SiC analogue.[13] Another approach avoids bulk materials. Tolbert *et al.* reported that polymer-templated porous silica utra-thin films (ca 30 nm thick) prepared by the evaporation-induced self-assembly method, can be converted to silicon by a vapour magnesiothermic reaction. Partial maintenance of the framework was observed where the walls and pores are over 10-25 nm in dimension, on the same order as the film thickness. [14] They proposed that this is a minimum structural feature size for retention of nanostructural regularity. In accord with previous results, silicon domain sizes on the order of ~13 nm were suggested. Mg_2Si formation was not reported. Whether this is the consequence of film strain that seems resistant to over-reduction even with an excess of Mg vapour is not well understood.

The challenge remains to find an effective porous silica → porous silicon conversion methodology which maintains nanostructural regularity for a wide variety of porous silica structures as bulk materials irrespective of morphology. Herein, we introduce a route described in Scheme 1 below, which employs Mg_xM_y intermetallics as the reductants to gently convert silica nanostructures such as SBA-15 into their silicon replicas. The morphological and nanostructural features of the mesoporous silica are retained in their silicon replica without triggering over-reduction.

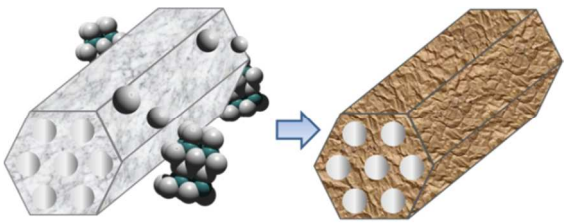

Scheme 1:
$2Mg_xM_y + xSiO_2 \rightarrow xSi + 2yM + 2xMgO$
(M = Sn, Sb, Si)

To realize the reaction in Scheme 1, the electronegativity of M in the intermetallic needs to be comparable or higher than that of silicon. In order to maintain the structure of the starting silica material, the enthalpy of the reaction needs to be weakly negative to prevent the highly exothermic reaction which gives rise to internally generated local heating that collapses the porous structure. Equations (2-6) show the reactions when Mg, Mg vapour, Mg_2Sn, Mg_3Sb_2 and Mg_2Si are used, respectively. The reactants and products are in their solid state unless otherwise specified.

$2Mg_{(s)} + SiO_2 \rightarrow Si + 2MgO$ …… (2) $\Delta H = -292$ kJ/mol

$2Mg_{(g)} + SiO_2 \rightarrow Si + 2MgO$ ……. (3) $\Delta H = -219$ kJ/mol

$Mg_2Sn + SiO_2 \rightarrow Si + Sn + 2MgO$…… (4) $\Delta H = -227$ kJ/mol

$2Mg_3Sb_2 + 3SiO_2 \rightarrow 3Si + 4Sb + 6MgO$ (5) $\Delta H = -102$ kJ/mol

$Mg_2Si + SiO_2 \rightarrow Si + Si^* + 2MgO$ … (6) $\Delta H = -221$ kJ/mol

The enthalpy changes per mole of silicon extracted from silica in the reactions (2 to 6) are calculated based on basic thermodynamic data.[15] Note that Si* represents the silicon phase that originates from Mg_2Si, which can be separated on the basis of density. The intermetallics, Mg_xM_y (M = Si, Sn, Sb) exhibit more positive enthalpy changes than pure Mg due to their increased lattice energy arising from the polarized Mg – M bond. Heat capacities of different reaction mixtures can be estimated with the Dulong-Petit equation (*c=3R/M,* where R is the gas constant, and M is the molar mass). The maximum temperature rises can therefore be calculated. They are 2131 °C for the SiO_2/Mg (1:1 in mass) mixture, 603 °C for the SiO_2/Mg_3Sb_2 (1:4 in mass) mixture and 1147 °C for the SiO_2/Mg_2Si (1:2 in mass) mixture under adiabatic conditions. The practical values will be less since the flowing argon gas carries away some heat and heat is also lost to the reaction container. The values shed light on the large difference in local reaction temperatures between different reduction reactions.

These reactions are effective because at elevated temperatures, Mg intermetallics sustain a measurable Mg vapour pressure which is naturally lower than that of Mg metal owing to the contribution of Mg-M bonding. Mg infusion into GaAs has been achieved using Mg_3Sb_2,[16] and Mg vapour pressures have been measured for Mg_2M (M = Ge, Si, Sn, Pb) between 600-900 °C, showing they increase in that order.[17] The lower concentration of Mg in the gas phase (*vis a vis* the metal) results in a slower reaction rate, which consequently allows more effective dissipation of local heating.[18] Differential scanning calorimetry (DSC) measurements were conducted to investigate reactions (2), (5), and (6) for a qualitative comparison, as depicted in **Figure 1**. Silica and the reductants were ground together and loaded into a Pt cup. The variance in the elemental Mg loading between the three measurements was kept within 2%. A large and early exothermic peak at 590 °C is observed for reaction (2) in accord with the enthalpy estimate above. The exothermic signatures observed for (5) and (6) are weaker and appear at higher temperatures of 660 °C and 700 °C, respectively. The shift in temperature is likely due to the lower Mg vapor pressures, coupled with mass transport effects. The results thus inspired us to use reactions (5) and (6) to deoxygenate silica under mild conditions that preserve the nanostructural integrity. We demonstrate here that Mg_2Si gives rise to better nanostructure retention at the temperature where magnesiothermic reduction occurs.

Syntheses of Mg_3Sb_2 and Mg_2Si were conducted by solid state reaction (see SI), and their purity confirmed by comparison of their X-ray diffraction (XRD) patterns to the JPDS database ([01-071-0404] and [01-075-0445] respectively). These intermetallic phases

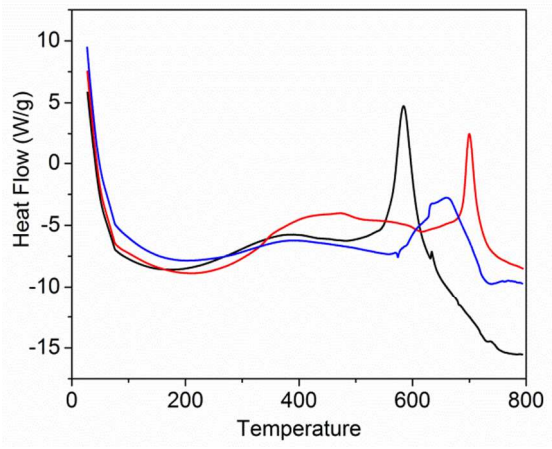

Figure 1. **Differential scanning calorimetry (DSC) under dynamic argon flow,** of Mg and SiO_2 (black curve, (eqn 2)); Mg_3Sb_2 and SiO_2 (blue curve, eqn 5) and reaction (6): Mg_2Si and SiO_2 (red curve, eqn (6)).

are active in the magnesiothermic displacement reactions described below. We chose SBA-15,[19] well-established mesoporous silica, as the target nanostructure for reduction to its silicon replica analogue. The SBA-15 samples and an excess of reductant (by ~ 25% in a molar ratio) were ground together intimately under an Ar atmosphere and pressed into a pellet under a pressure of 10^4 N/cm^2, prior to reaction at 700°C for 5 hrs (see SI for details). At this pressure, the pores in SBA-15 remain intact. Based on the measured densities of the pellets and the densities of solid components, these pellets have about 30% porosity. Within the pellets, magnesium vapor released from the decomposition of the intermetallic will react with the nearest neighbour silica particles. Mass transfer is of critical importance in this system, which is optimized to minimize Mg diffusion length while maintaining pathways for transport. We estimate that an Mg atom would have to travel a length scale of microns at most, given that the particle size of the SBA-15 is on this order, and that the particles are relatively well packed. This gives rise to good reaction homogeneity. Three different reactions were explored for comparison. Micron-sized particles of SBA-15 shown in **Figure 2a** were reacted with Mg_3Sb_2 to form a silicon material referred to as Si-Mg_3Sb_2. Nano-sized SBA-15 was prepared as previously reported,[20] and reacted with Mg_2Si to form Si-Mg_2Si. To provide a reference point, micron-sized SBA-15 particles were also reacted with Mg powder in a pellet (Mg/SiO_2 mass ratio: 1 to 1) at 650°C for 5 hrs under Ar to form Si-Mg. The SEM images in **Figure 2a and b** show the difference in morphology between SBA-15 before and after conversion. Significant residual SBA-15 crystallites are evident due to incomplete reduction. These are easily identified because of their characteristic hexagonal morphology, (examples are highlighted in the red boxes). This is similar to that previously reported for other porous silicas.[12] More importantly, reduction with Mg causes the discrete SBA-15 crystals to merge into large macroporous silicon agglomerates. The extensive morphology change is akin to a "welding process", which indicates a local temperature above the melting point of the silicon micron-rods (~1400°C) was achieved despite the set temperature of 650°C. This confirms the results of the above calculation on the temperature rise of the reaction mixture. This was so high that the reaction mixture pellet burst into powder after heating. The reaction is comparable to the well-known solid state metathesis processes[21,22] that are also highly exothermic. The reaction of micron-sized SBA-15 with the intermetallic reducing agent Mg_3Sb_2 produced different results. The pellet of the reaction mixtures remains intact after the reaction, and the excess Mg_3Sb_2 and residual MgO (indicated by the XRD pattern,

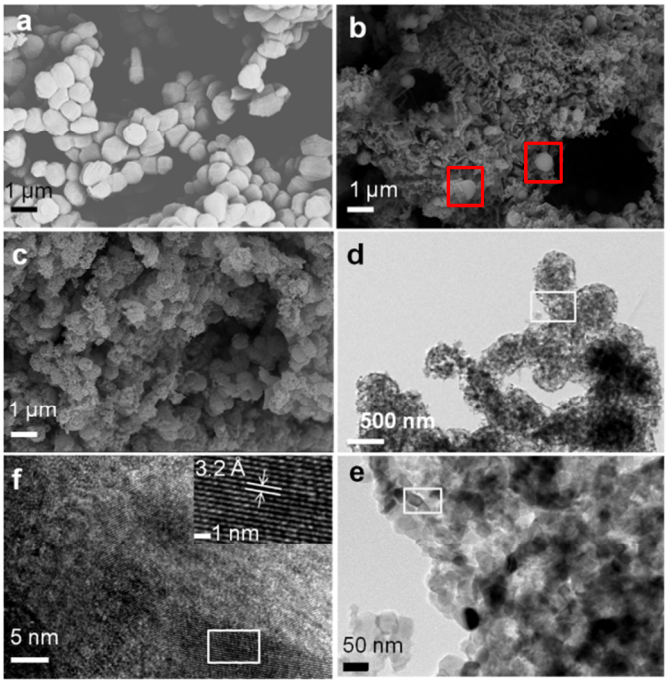

Figure 2. **The reaction of bulk SBA-15 silica with Mg vapour *vs* reaction with intermetallic Mg_2Sb_3 monitored by electron microscopy.** SEM images of a) bulk silica SBA-15; b) its collapsed silicon product, Si-Mg**,** formed by reduction with Mg; c) its porous silicon product, Si-Mg_3Sb_2, formed by reduction with Mg_2Sb_3. d) TEM image of porous Si-Mg_3Sb_2; e) and f) are TEM images showing expansions of the area marked with a box in d) and e), respectively.

Figure S1) was easily leached out from the crushed pellet with a mixture of HCl/HNO_3. The particle morphology of SBA-15 is much better maintained under these conditions to form the silicon product whose representative morphology is shown in the SEM image (**Figure 2c**). These Si particles exhibit a characteristic surface morphology which appears very roughened, in contrast to the smooth solid surface of the SBA-15 particles shown in **Figure 2a**. A thorough inspection of the sample confirmed that no SBA-15 particles remain. The crystalline nature of the Si-Mg_3Sb_2 is confirmed by the well resolved peaks in its wide angle XRD pattern (**Figure S2**). The coherence length is calculated to be approximately 25 nm, much less than that of Si-Mg (>40 nm). The non-Gaussian lineshape of the pattern indicates that there are in fact, two contributions to the line width, which were deconvoluted into a sharper more crystalline component with a coherence length of 25 nm, and a broader component with a coherence length of ~ 6 nm. This indicates that Si-Mg_3Sb_2 was formed at a local reaction temperature high enough to melt silicon domains less than 20 nm, but low enough not to melt ones larger than 20 nm. The local temperature is lower than that of the Mg vapour reduction, as judged by the silicon domain sizes**.** Thus, given sufficient reaction time, the complete conversion of SiO_2 to Si is readily achieved without over-reduction using the intermetallic. This is a significant advantage, since an excess of Mg_3Sb_2 ensures that complete reduction of silica stops at the formation of silicon. However, the highly ordered porous structure of the silica precursor is not maintained on the nanoscale. As in the case of Si-Mg, this is indicated by the absence of a well resolved peak in the low angle XRD pattern, (**Figure 3a,b**) showing there is no long range order. TEM analysis confirmed this finding. The overall loosely connected structure of the SBA-15 derived silicon particles is shown in the TEM image in **Figure 2d**, which is representative of the overall sample based on extensive mapping.

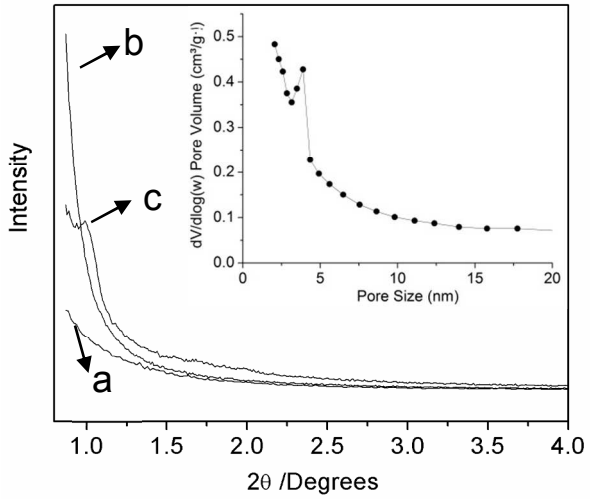

Figure 3. **Physical characterization of the silicon replicas formed by reaction of SBA-15 with Mg, Mg_2Sb_3 (Si-Mg_3Sb_2) and Mg_2Si (Si-Mg_2Si).** Low angle XRD pattern of a) Si-Mg b) Si-Mg_3Sb_2; c) Si-Mg_2Si. Inset: pore size distribution of Si-Mg_2Si.

Expansion of the region outlined by the white box is shown in the image in **Figure 2e,** with higher magnification and the accompanying HRTEM image shown in **Figure 2f**. Evident are silicon domains about 20 nm in dimension that exhibit clear (111) crystalline fringes (d: 0.32 nm), crystallized within larger particles (**Figure 2f**) indicative of partial melting as suggested by the XRD.

To preserve the nanoporous long range order inherent in SBA-15, we reacted nano-sized SBA-15 together with the intermetallic Mg_2Si which has a reported vapour pressure of Mg of 1 mmHg at 790ºC.[17] After reduction and HCl (2M) treatment, two silicon phases remain, as described by reaction (6): one is the nano-phase from the reduction of the nano-SBA-15 silica that we term Si-Mg_2Si. The other is the bulk Si phase released from reaction of the micron-sized Mg_2Si reductant. Their separation was achieved by a sonication-precipitation method due to their vastly different particle sizes and density. After the mixture was sonicated for 10 hrs and allowed to stand for 24 hrs, the heavier bulk silicon phase settled and the lighter, suspended silicon nanorods were collected by simple centrifugation. The Si-Mg_2Si was examined by SEM and analysed by EDX (**Figure 4b; Figure S3**). Mapping under the microscope confirmed that the major product was nanorod Si-Mg_2Si, although a few large particles from contamination of bulk Si arising from the reductant were still visible, which dominated the XRD pattern. EDX indicated the nanorods were primarily Si, with some residual oxide as expected from surface passivation. The nanorod morphology is well maintained after reduction to Si-Mg_2Si; moreover, the well resolved peak in the low angle XRD pattern reveals the long range order is also preserved (**Figure 3c**). The peak is assigned as the (100) plane inherited from the original hexagonal structure. The inherent porosity was confirmed by nitrogen absorption measurements of Si-Mg_2Si which revealed a specific Brunauer-Emmett-Teller (BET) surface area of 300 m^2/g and a total Barrett-Joyner-Halenda (BJH) specific pore volume of 0.30 cm^3/g (see **Figure S4**, SI for details). If the parent SBA-15 (620 m^2/g) were topotactically converted to Si, a surface area of 530 m^2/g would be predicted in light of the density difference of the frameworks (2.3 cc/g for Si; 2.0 cc/g for mesoporous SiO_2). Thus a sizable fraction of the silica structural porosity is retained in the transformation to silicon, although some is lost as expected. The pore size distribution shown in **Figure 3** (inset) indicates mesopores of 4 nm in dimension, in accord with the expected shrinkage of the 7 nm pores in SBA-15 silica on densification. To further confirm that it is the silicon that

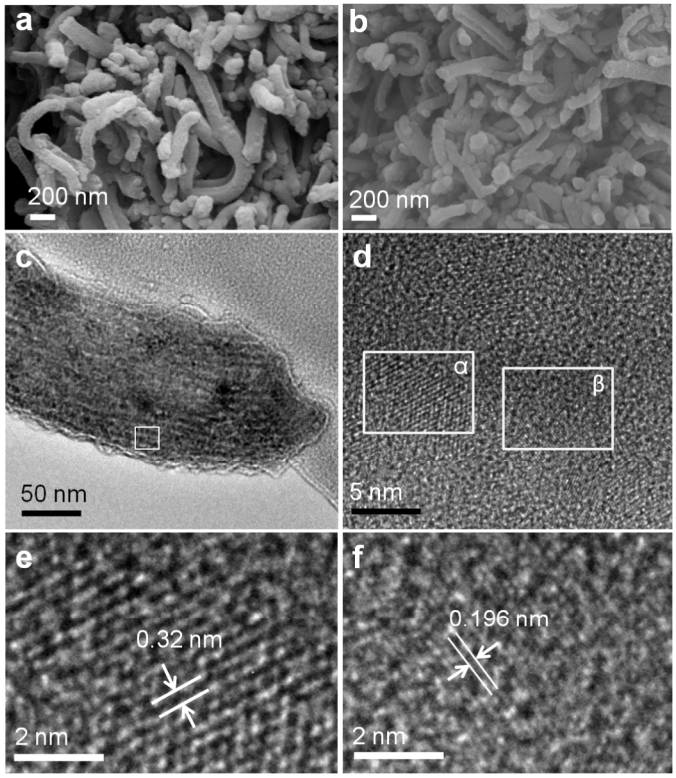

***Figure 4*. The reaction of nano-sized SBA-15 silica with Mg_2Si probed by electron microscopy.** SEM images of a) SBA-15 silica nanorods; b) nanoporous silicon (Si-Mg_2Si). Representative TEM images of nanoporous Si-Mg_2Si; c) at low magnification; d) a high resolution image of the area marked with a box in c); e,f) high resolution TEM images that correspond to the areas in d) are marked by the boxes α and β, respectively.

constitutes the nanoscopic regularity, we carried out high resolution TEM studies. Representative images (Figure 4c, and expansions in Figure 4d,e,f) show that discrete silicon nanocrystallites with characteristic *d* spacings of 0.32 nm or 0.196 nm ((111) and (220), respectively) form the wall structure in the well preserved nanoporous material. The size of the nanocrystallites is only ~ 5 nm, substantially smaller than the silicon domains obtained by the other magnesiothermic chemistry, and also less than 13 nm as previously reported.[12,14] This indicates the local reaction temperature must be much lower than the melting temperature of silicon. During reduction, magnesia particles and liberated silicon nanocrystallites are formed in concert. Nonetheless, the SBA-15 nanostructure is still maintained after magnesia removal.

Conclusions

By employing mild magnesiothermic displacement reactions via an intermetallic as a source of Mg, mesoporous SBA-15 silica can be converted to its silicon replica with retention of morphology and the original silica nanostructure. Over-reduction and structural degradation observed in previously reported magnesiothermic reactions are inhibited. To our knowledge, this is the first time that the structural features of bulk (as opposed to thin film) SBA-15 silica are inherited in its silicon replica on the nano-level. Our work sheds light on new reduction methodologies that can be conducted in a well-controlled manner and which are applicable to a range of silicas with framework mesoporosity.

Notes and references

[a] University of Waterloo, Department of Chemistry, Waterloo, Ontario, N2L 3G1, Canada, Email: lfnazar@uwaterloo.ca
[b] McMaster University, Department of Chemistry and Canadian Facility for Electron Microscopy, Hamilton, Ontario, L8S 4L8, Canada.
†Current address: Department of Chemistry, Oregon State University, Corvallis OR, USA.

Acknowledgments L.F. Nazar gratefully acknowledges the financial support of NSERC through its Discovery Grant and Canada Research Chair programs, and the facilities provided by the Canadian Centre for Electron Microscopy. LFN and XJ thank Dr. Liang (UW) and Mr. Z. Xing (OSU) for technical support.

Electronic Supplementary Information (ESI) available: Syntheses of the intermetallics, and SBA-15 [15,16], preparation of the nanoporous silicon, and BET and EDX data. See DOI: 10.1039/c000000x/

References

1 D.Y. Zhao, P.D. Yang, Q.S Huo, B.F. Chmelka, G. D. Stucky, *Current Opinion Sol. Stat Sci Mat Sci*., 1998, **3**, 111; N.D. Petkovich, A. Stein, *Chem. Soc., Rev*., 2013, **42**, 3721; A. H. Lu, F. Schueth, *Adv. Mater*., 2006, 18, 1793.
2 M. D. Kelzenberg, S. W. Boettcher, J. A. Petykiewicz, D. B. Turner-Evans, M. C. Putnam, E. L. Warren, J. M. Spurgeon, R. M. Briggs, N. S. Lewis, H. A. Atwater, *Nature Mater.* 2010, **9**, 239.
3 A. I. Hochbaum, R. Chen, R. D. Delgado, W. Liang, E. C. Garnett, M. Najarian, A. Majumdar, P. Yang, *Nature* 2007, **451**, 163.
4 J. Cho, *J. Mater. Chem*., 2010, **20**, 4009.
5 H. Kim, M. Seo, M.-H. Park, J. Cho, *Angew. Chem. Int. Ed.* 2010, **49**, 2146.
6 B. Tian, T. J. Kempa, C. M. Lieber, *Chem. Soc. Rev.* 2009, **38**, 16.
7 Z. Huang, N. Geyer, P. Werner, J. de Boor, U. Gösele, *Adv. Mater.* 2011, **23**, 285.
8 H. Kim, J. Cho, *Nano Lett.* 2008, **8**, 3688.
9 M. Nagamori, I. Malinsky, A. Claveau, *Metallur. Trans. B* 1986, **17B**, 503.
10 F.G. Reshetnikov, E.N. Oblomeev, *Sov. Atom. Ener.* 1957, **2**, 561.
11 Z. H. Bao et al., *Nature* 2007, **446**, 172.
12 Y. Yu, L. Gu, C. Zhu, S. Tsukimoto, P. A. van Aken, J. Maier, *Adv. Mater.* 2010, **22,** 2247.
13 Y. Shi, F. Zhang, Y.-S. Hu, X. Sun, Y. Zhang, H. I. Lee,† L. Chen, G. D. Stucky, *J. Am. Chem. Soc*. 2010, **132**, 5552.
14 E. K. Richman, C. B. Kang, T. Brezesinski, S. H. Tolbert, *Nano Lett.* 2008, **8**, 3075.
15 W. M. Haynes, D. R. Lide, Handbook of Chemistry and Physics, 91st ed. Chemical Rubber Company, 2010.
16 M. Belasco, Texas Instruments Inc., US Patent 3,357,872 (1967).
17 E. N. Nikitin, N. Rozyev, *Russian Journal of Applied Chemistry*, 1970, **43**, 2093.
18 B. Yuan, T. H. Okabe, *J. Alloys and Comp.* 2007, **443**, 71.
19 D. Zhao, J. Feng, Q. Huo, N. Melosh, G. H. Fredrickson, B. F. Chmelka, G. D. Stucky, *Science* 1998, **279**, 548.
20 X. Ji, K.T. Lee, M. Monjauze, L. F. Nazar, *Chem. Commun.* 2008, 4288.
21 R. A. Cutler, K. M. Rigtrup, *J. Am. Ceram. Soc.* 1992, **75**, 36.
22 S. K. Bux, M. Rodriguez, M. T. Yeung, C. Yang, A. Makhluf, R. G. Blair, J.-P. Fleurial, R. B. Kaner, *Chem. Mater.* 2010, **22**, 2534.

